Dendritic growth velocities in undercooled melts under static magnetic fields

Jianrong Gao[1], Jia Liu[1], Andrew Kao[2], Koulis Pericleous[2]

[1] Key Laboratory of Electromagnetic Processing of Materials (Ministry of Education)
Northeastern University Shenyang 110819, People's Republic of China
[2] Centre of Numerical Modelling and Process Analysis, University of Greenwich
London SE10 9LS, United Kingdom

Corresponding author: jgao@mail.neu.edu.cn

Abstract
Dendritic growth in undercooled melts has been an interesting topic for metallurgists, physicists and mathematicians. In recent years, attention has been focused on the effects of melt flow on dendritic growth. Significant thermoelectric currents form in undercooled growth due to the presence of relatively large thermal gradients. Numerical simulations showed that the application of a static magnetic field exerts a complex influence on melt flow due to Lorentz force, damping and thermoelectrically driven convection, affecting growth kinetics in undercooled metallic melts. To verify the simulated results, bulk melts of high purity nickel were undercooled using the glass fluxing technique under static magnetic fields of up to 6 T. A high-speed camera was used for *in situ* monitoring of the recalescence process of the undercooled samples. The dendritic growth velocities at different melt undercoolings were calculated by simulating the recorded images of the recalescence process. The measured data confirms the predicted effect of heat and mass transport through thermoelectric magnetohydrodynamics flow on dendritic growth.

Key words: Dendritic growth; Undercooling; Static magnetic fields; Thermoelectric magnetohydrodynamics

Introduction

Dendritic growth is often observed in solidification of undercooled metallic melts. It determines the final grain sizes and solute segregation patterns of metal castings [1]. Fundamentally, it represents a non-linear and a non-equilibrium process [2]. For these reasons, it has aroused common research interest in the fields of metallurgy, materials physics and computational mathematics. Since the pioneer work by Ivantsov in late 1940's [3], theoretical efforts have been made to predict the relationships between melt undercooling, the tip radius and tip velocity of a growing equiaxed dendrite (see Ref. [4] and references therein). In recent years, the effect of melt flow on dendritic growth aroused novel research interest because it is largely responsible for a discrepancy between theory and experiment for low undercoolings [5-6]. Magnetic fields are commonly used as a tool for controlling of melt flow in metallic melts. An alternating current (AC) magnetic field with high frequency can produce intensive melt flow known as electromagnetic stirring [7], whereas a static magnetic field typically introduces electromagnetic damping forces and thus can effectively reduce or remove fluid flow [8,9]. However, the role of the static magnetic field is not limited to damping, especially close to the solid front. The interaction of the static magnetic field with natural and inherent thermoelectric currents produces the phenomenon of thermoelectric magnetohydrodynamics (TEMHD) [10-12] leading to intensive melt flow around the primary tip, and secondary or higher order arms of a dendrite growing at significant undercoolings. Such opposing effects of the static magnetic field provide a cheap way for quantitative terrestrial studies of the effect of melt flow on dendritic growth when compared with space experiments [5].
Dendritic growth kinetics in pure nickel has been intensively studied over the past decades (see a review in Ref. [13]). An impurity effect has been considered to account for the remaining discrepancy between the theory of dendritic growth and the experimental data at low undercoolings [6]. A recent experimental study on elemental nickel of 99.99% purity revealed a U-shaped magnetic field dependence at low melt undercoolings [14]. However, the effect of impurities on the dendritic growth velocities in the presence of TEMHD is unclear. This paper presents numerical simulations of the damping and thermoelectric effects of the static magnetic fields during melting and solidification of a glass-fluxed metallic sample, followed by measured data of dendritic growth velocities of nickel of higher purity under static magnetic fields and finally a comparison between the prediction of the numerical simulations and the experimental data.

Numerical Models

Numerical simulations were carried out to simulate the melt flow during natural cooling of an inductively melted spherical nickel sample of 6 mm in diameter under a static magnetic field. The details of the method can be found elsewhere [8]. It was found that the imposition of a static magnetic field of 0.5 T or more can damp melt flow in the nickel sample effectively. In the absence of a static magnetic field, the AC magnetic field used for induction melting produces strong turbulent flow of the magnitude of 0.1-1 m/s. As illustrated in Fig. 1, the turbulent flow is suppressed

and the flow velocity is reduced to less than 0.01 m/s under the influence of a 6 T static magnetic field. There is a thermal gradient along the z direction, namely the direction of the static magnetic field. This gradient can be attributed to radiation cooling of the sample in the absence of electromagnetic stirring. The calculated gradient is in reasonable agreement with a measured gradient of 2.5 K/mm on an inductively melted Ni-Sn eutectic sample of the same size.

The numerical simulation of TEMHD flow during dendritic growth from an undercooled melt is illustrated in Fig. 2. The figure shows the complex TEMHD flow structure that forms in the presence of an arbitrarily low static magnetic field. TEMHD creates flow circulations about the growth direction of the primary tip. For tangential tips, the flow is tilted and the corresponding flow patterns become complex, which grow in a direction normal to the static magnetic field. Such flow patterns will have different influences on the dendritic tip kinetics (tip radius and tip velocity) and eventually lead to very complex growth morphology [10,11]. In general, the TEMHD flow is localized and the flow structure and magnitude are highly dependent on the thermophysical properties of the crystalline material, on the direction and intensity of the magnetic fields and on the growth conditions of the dendrite (undercooling and chemical composition) as well.

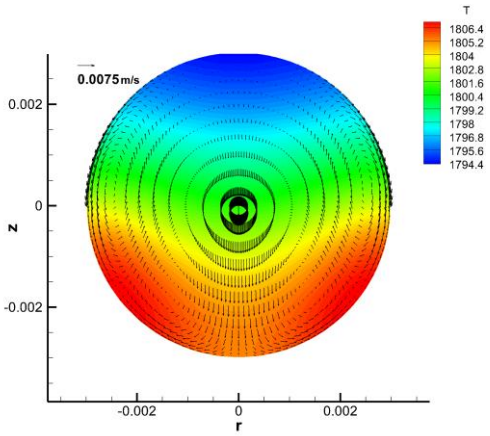

Fig. 1: Simulated flow velocity and temperature in a nickel sample inductively melted under a 6 T static magnetic field along the z direction. The r and z are distances away from the center of the sample in m. Temperature is in K.

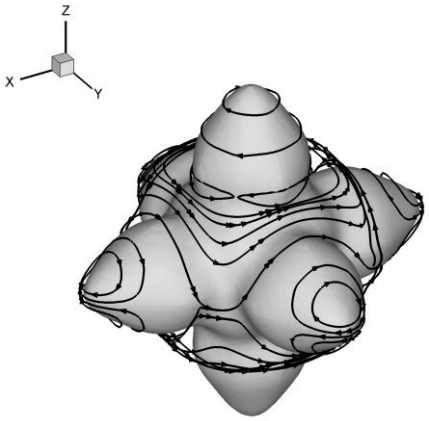

Fig. 2: Simulated flow structure of TEMHD around an equiaxed dendrite growing from an undercooled melt under an arbitrarily low static magnetic field (taken from ref. [11]).

In-situ Observations

Electromagnetic levitation is a popular method for high undercooling of a bulk melt. A levitated sample usually rotates and needs to be cooled using an inert gas jet. Glass fluxing offers access to comparable undercoolings of non-reactive metallic melts. But, it allows samples to be cooled without the use of the noble inert gas. The cost of the measurement is reduced and the experimental time is shortened as only a single or a few samples are required [13]. In the present work, it was combined with induction melting for measurements of dendritic growth velocities in undercooled melts under static magnetic fields. As shown in Fig. 3, the experimental set-up used has four key parts: a radio frequency vacuum induction melting furnace, a superconducting magnet, a high-speed camera, and a single-color pyrometer. The superconducting magnet has a room-temperature cylindrical bore of 300 mm in diameter and offers static magnetic fields of intensities up to 6 T. The high-speed camera was not focused directly onto the sample surface, but was focused onto an image of the sample projected into a prism at a distance of about 0.7 m (see Fig. 3b). The camera has a maximum frame rate of 125,000 fps and a two-dimensional resolution of 100 $\times$ 100 μm^2 (128 $\times$ 32 pixel). This resolution is sufficient for measurements of growth velocities ranging from 0.1 m/s to 100 m/s. The pyrometer was used for monitoring the surface temperature of the sample at a sampling rate of 100 Hz with an accuracy of $\pm$ 6 K. The sample was nickel of 99.999% purity with a mass of 1.0 g. Before the measurements, the vacuum chamber of the induction melting furnace was evacuated to a pressure of 5×10^{-3} Pa, and backfilled with argon of 99.999% purity to a pressure of 5×10^{4} Pa. The measurements were started with no static magnetic field at first. The sample was heated, melted and overheated inductively under the protection of the argon atmosphere. The overheating of the sample was carefully controlled by tuning the power to the coil to produce a desired undercooling during the subsequent cooling. After the sample was held in the overheated state for one or more minutes, the heating power was reduced to about 14% of the initial value to let the sample cool at a rate of about 20 K/s. Crystal nucleation in the undercooled sample was not controlled using an external trigger. Very often nucleation occurred on the lower surface of the sample. Recalescence followed due to rapid release of latent heat. The advancing of the recalescence front on the sample surface was

monitored and recorded using the high-speed camera. The melting and solidification cycle was repeated 20 to 40 times to produce a wide spectrum of undercooling. After the measurements under no static magnetic field, the superconducting magnet was ramped to a magnetic field of 1 T, 2 T, 3 T, 4 T, 5 T and 6 T in sequence. Under each magnetic field, the same measurements were conducted by repeating the melting and solidification cycle of the sample at least 20 times. The recorded images were analyzed using a Pov Ray software program (V 3.6) to determine dendritic growth velocities during recalescence. The details of the method for image analysis can be found elsewhere [13].

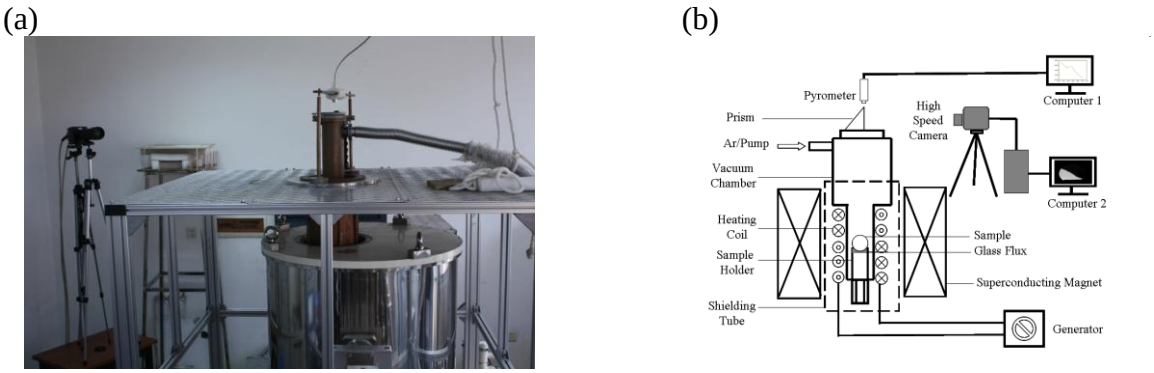

Fig. 3: Bird's eye view (a) and schematic diagram (b) of experimental set-up used for measurements of dendritic growth velocities under static magnetic fields.

The measured growth velocities are plotted in Fig. 4 as a function of undercooling. The data measured under each static magnetic field shows a power law before a critical undercooling of ΔT_{crit} = 165 K is achieved. The growth kinetics shows a negative deviation from the power law at higher undercoolings. Such observations are in agreement with our recent measurements on a pure nickel sample of lower purity [14]. To investigate the effect of melt convection on the dendritic growth kinetics, the measured data at undercoolings below 165 K was fitted to different power laws and normalized with respect to a maximum for a given undercooling. The normalized growth velocities are shown in Fig. 5 as a function of the intensity of the static magnetic fields. For undercoolings below 100 K, the normalized growth velocities decline slightly or remain constant with increasing intensity of the static magnetic fields. They peak up at a critical magnetic field of 4 T and show a declining tendency at higher static magnetic fields. The dependences of the normalized growth velocities become indistinguishable for undercoolings of 100 K or above (in consideration of a total error of about 20 % in the measurements and in the power law fittings). Such a complex dependence is different from the U-shaped dependence observed for the normalized growth velocities of the nickel sample of lower purity [14]. Despite this difference, the undercooling range where the static magnetic fields have a clear effect on dendritic growth velocities is essentially the same.

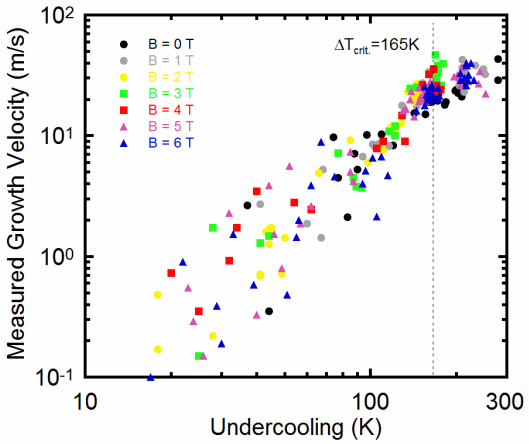

Fig. 4: Measured dendritic growth velocities of pure nickel as a function of undercooling. The dotted line shows a critical undercooling of 165 K for deviations from a power law.

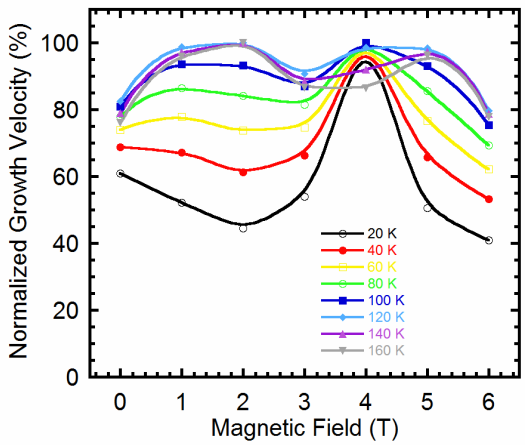

Fig. 5: Normalized dendritic growth velocities of pure nickel as a function of the intensity of static magnetic fields at undercoolings below 165 K. The curves are a guide to the eye.

Discussion and Concluding Remarks

The present measurements show complex effects of the static magnetic fields on dendritic growth velocities of pure nickel. The constant or slightly reduced growth velocities at low and high field sides can be attributed to the dominance of the damping effect over the TEMHD effect. The peak growth velocities observed at the critical magnetic field of 4 T can be related to the strongest TEMHD flow near the dendritic tip. These observations are in agreement with the earlier numerical simulation of the TEMHD flows during dendritic growth [11].

The present results also suggest that there is an effect of impurities on the dendritic growth velocities of pure nickel. The lower impurity level of the present nickel samples leads to the complex magnetic field dependence of the dendritic growth velocities with respect to the U-shaped dependence observed in the lower purity sample. The complex magnetic field dependence reflects the intrinsically complex TEMHD flows in dendritic growth. The higher impurity level of the previous nickel sample in recent measurements [14] may further increase the intrinsic complexity of the TEMHD phenomenon during dendritic growth from the undercooled melt. TEMHD flow is highly dependent on the local Seebeck coefficients at the solid/liquid interface. Impurities, which have a tendency to congregate at the interface, may modify these values significantly, in effect acting as semiconductor-like dopants [15]. The higher impurity level of the previous sample [14] brings about a clear and remarkable depression of the growth velocities at low fields, which may be due to secondary TEMHD flows that have not yet been considered. But fundamentally this difference is rooted in interactions between solute rejection and melt convection. On the other hand, the higher impurity level of the previous sample [14] would also modify the intensities of the TEMHD flows by changing thermophysical/thermoelectric properties of liquid and solid phases. The critical magnetic field will be dependent on the thermophysical/thermoelectric properties. Thus, this second impurity effect may be responsible for the increase of the critical magnetic field. For a better understanding of the impurity effect, analytical and numerical modellings of the melt flow effect and the impurity effect on dendritic growth are under the way.

Acknowledgment

The work is financially supported by the National Natural Science Foundation of China (51071043 and 51211130113), the Fundamental Research Funds for Central Universities (N09050901 and N130509001), and the Royal Society International Exchanges Scheme - 2011 China Costshare (NSFC). The authors thank D. M. Herlach, P. K. Galenko and D. V. Alexandrov for helpful discussion of experimental data. The authors are indebted to V. Bojarevics for offering the computer code for magnetohydrodynamics modeling. The authors are grateful to C. Yang, Y. J. Zhang, X. T. Deng, J. C. Jin, D. Xiang and H. L. Zhao for assistance in experimental work. The authors also thank S. Binder for providing computer program for image analysis.

References

[1] D. M. Herlach (2012), Mater. Sci. Eng. Rep. 12, 177-272
[2] J. S. Langer (1980), Rev. Mod. Phys. 52, 1-28
[3] G. P. Ivantsov (1947), Dokl. Akad. Nauk SSSR 58, 567-569
[4] R. Trivedi, W. Kurz (1994), Inter. Mater. Rev. 39, 49-74
[5] M. E. Glicksman, M. B. Koss, E. A. Winsa (1994), Phys. Rev. Lett. 73, 573-576
[6] O. Funke, G. Phanikumar, P. K. Galenko, L. Chernova, S. Reutzel, M. Kolbe, D. M. Herlach (2006), J. Cryst. Growth 297, 211-222
[7] S. Berry, R. W. Hyers, B. Abedian, L. M. Racz (2000), Metall. Mater. Trans. B 31, 171-178
[8] V. Bojarevics, K. Pericleous (2003), ISIJ Inter. 43, 890-898
[9] H. Yasuda, I. Ohnaka, Y. Ninomiya, R. Ishii, S. Fujita, K. Kishio (2004), J. Cryst. Growth 260, 475-485
[10] A. Kao, K. Pericleous (2012), Magnetodydrodynamics 48, 361-370.
[11] A. Kao, K. Pericleous (2012), J. Algorithms & Comp. Technol. 6, 173-202
[12] X. Li, Y. Fautrelle, Z. Ren (2007), Acta Mater. 55, 3803-3813
[13] J. Gao, Z. N. Zhang, Y. K. Zhang, C. Yang (2012), in: Solidification of Containerless Undercooled Melts, edited by D. M. Herlach and D. M. Matson, Weinheim, Wiley VCH, 281-303.
[14] J. Gao, M. K. Han, P. K. Galenko, D. V. Alexandrov, to be published.
[15] J. P. Garandet, T. Alboussiere (1999), Prog. Cryst. Growth Charact. Mater. 38, 73-132.